Journal of Materials Science and Chemical Engineering, 2022, 10, 30-41
https://www.scirp.org/journal/msce
ISSN Online: 2327-6053
ISSN Print: 2327-6045

Experimental and Computational Study of the Microwave Absorption Properties of Recycled α-Fe_2O_3/OPEFB Fiber/PCL Multi-Layered Composites

Ebenezer Ekow Mensah[1*], Raba'ah Syahidah Azis[2,3], Zulkifly Abbas[2]

[1]Department of Integrated Science Education, Faculty of Science Education, Akenten Appiah-Menka University of Skills Training and Entrepreneurial Development, Mampong, Ashanti, Ghana
[2]Department of Physics, Faculty of Science, Universiti Putra Malaysia, Selangor, Malaysia
[3]Institute of Advanced Materials, Universiti Putra Malaysia, Selangor, Malaysia
Email: *ebemensek@yahoo.co.uk, *ebenekowmensah@aamusted.edu.gh, rabaah@upm.edu.my, za@upm.edu.my

How to cite this paper: Mensah, E.E., Azis, R.S. and Abbas, Z. (2022) Experimental and Computational Study of the Microwave Absorption Properties of Recycled α-Fe_2O_3/OPEFB Fiber/PCL Multi-Layered Composites. *Journal of Materials Science and Chemical Engineering*, **10**, 30-41.
https://doi.org/10.4236/msce.2022.103003

Received: January 31, 2022
Accepted: March 25, 2022
Published: March 28, 2022

Abstract

The aim of this study was to fabricate multi-layered recycled α-Fe_2O_3/OPEFB fiber/PCL composites for microwave absorbing applications in the 1 - 4 GHz frequency range. The multi-layered composites were 6 mm thick and each consisted of a 2 mm thick layer of recycled α-Fe_2O_3/PCL composites at various loadings (5 wt% - 25 wt%) of 16.2 nm recycled α-Fe_2O_3 nanofiller, placed between two layers of 2 mm thick OPEFB fiber/PCL composites blended at a fixed ratio of 7:3. The real (ε') and imaginary (ε'') components of the relative complex permittivity were measured using the open-ended coaxial probe technique and the values obtained were applied as inputs for the Finite Element Method to calculate the reflection coefficient magnitudes from which the reflection loss (RL) properties were determined. Both ε' and ε'' increased linearly with recycled α-Fe_2O_3 nanofiller content and the values of ε' varied between 3.0 and 3.9 while the ε'' values ranged between 0.26 and 0.64 within 1 - 4 GHz. The RL (dB) showed the most prominent values within the 1.38 - 1.46 GHz band with a minimum of -38 dB attained by the 25 wt% composite. Another batch of minimum values occurred in the 2.39 - 3.49 GHz range with the lowest of −25 dB at 2.8 GHz. The recycled α-Fe_2O_3/OPEFB fiber/PCL multi-layered composites are promising materials that can be engineered for solving noise problems in the 1 - 4 GHz range.

Keywords

Multi-Layered Composites, Recycled α-Fe_2O_3, Reflection Loss, OPEFB Fiber,

Relative Complex Permittivity

1. Introduction

The advancements in contemporary wireless electronics at low RF/microwave frequencies have intensified the electromagnetic interference (EMI) problem for several electronic devices having civilian and military applications. The situation has given rise to the development of a wide range of absorber-based solutions aimed at offering electromagnetic compatibility to enhance the reliability and quality of these sophisticated electronic devices. Generally, the materials employed in EMI absorbing applications can be classified as dielectric, magnetic and magneto-dielectric (hybrid), with ferrites such as soft magnetic spinel ferrites [1] [2] [3], hard U and M-type ferrites [4] [5] being among the most widely used magnetic materials. Ferrite materials are known to be chemically stable and also have higher saturation magnetization and magnetic loss [6] as well as larger electrical resistivity but lack the appropriate balance of low density and high dielectric loss properties.

One approach which many researchers have exploited in recent years to reduce the effect of these limitations is to combine ferrite materials with carbon-based materials or conducting polymers to synthesize hybrid absorbers which have shown remarkable absorption characteristics over a wide range of microwave frequencies [4] [7] [8] [9] [10]. However, the replication of this approach using carbon bio-based materials and non-conducting polymers has received very little attention. For instance, carbon bio-based materials from agricultural residues such as oil-palm empty fruit bunch (OPEFB) fiber could serve as an inexpensive and green substitute to the frequently used carbon nanotubes and graphene oxides. A recent study by Abdalhadi *et al.* [11] reported that 100 μm grain-sized compacted OPEFB fiber had high dielectric loss values which ranged between 0.57 and 0.61 in the 1 - 4 GHz range. Additionally, OPEFB fiber is biodegradable, lighter and can be easily melt-blended with ferrites and non-conducting polymers such as polycaprolactone (PCL) [12].

Generally, the preparation of ferrite materials of different morphologies is often associated with a variety of expenses [13] [14] which ultimately make the materials relatively expensive. Recently, α-Fe_2O_3 (a corundum-type ferrite) was reportedly recovered from recyclable mill scale steel waste [15] [16] and the dielectric loss properties were enhanced [17] through processing techniques which were cheap and friendly to the environment. Recycled α-Fe_2O_3 could therefore be considered as a cheaper alternative to the most frequently used ferrites while at the same time saving the environment.

Moreover, when hybrid composites are employed as single-layered structures, they act as single barrier absorbers and are thus limited by the number of absorption assembly. Therefore multi-layered absorption structures [18] [19] [20]

are designed to increase the absorption assembly with the view to improving the microwave absorption capacities of the composites. However, there is no information currently available on multi-layered absorbers based on recycled α-Fe_2O_3, OPEFB fiber and PCL composites.

In this current work, recycled α-Fe_2O_3/OPEFB fiber/PCL multi-layered composites were fabricated using recycled α-Fe_2O_3/PCL and OPEFB fiber/PCL composites. The recycled α-Fe_2O_3/PCL composites consisted of various loadings (5 wt% - 25 wt%) of 16.2 nm recycled α-Fe_2O_3 nanofiller while the OPEFB fiber/PCL composites were blended at fiber to PCL ratio fixed at 7:3. The open-ended coaxial (OEC) probe method was then used to determine the relative complex permittivity properties which were subsequently used as inputs in the Finite Element Method to calculate the reflection coefficient magnitude in the L-S band from which the reflection loss performances of the composites were evaluated. A simulation of the x-component (V/m) of the electric field distribution within the composites was subsequently carried out to further assess their absorbing properties.

2. Materials and Methods

2.1. Preparation of Recycled α-Fe_2O_3/PCL Composites

5 wt% of 16.2 nm recycled α-Fe_2O_3 nanopowder, prepared from industrial mill scale waste using methods described by Mensah *et al.* [17], was mixed with 95 wt% PCL (Sigma-Aldrich, St. Louis, MO, USA) in a Brabender Extruder (Brabender GmbH & Co. KG, Duisburg, Germany) for 15 minutes at 65˚C to synthesize the composite of total mass 25 g. The procedure was repeated using 10 wt%, 15 wt%, 20 wt% and 25 wt% of the nanofiller and 90 wt%, 85 wt%, 80 wt% and 75 wt% of PCL respectively. 8.33 g of each of the composites were then placed in 6 cm × 3.6 cm × 0.20 cm molds and hot-pressed at a pressure of 110 kg/cm^2 into flat blocks.

2.2. Preparation of OPEFB Fiber/PCL Composite

Using the procedure outlined in Abdalhadi *et al.* [11], purified OPEFB (Ulu Langat Oil Palm Mill, Dengkil, Selangor, Malaysia) was milled into 100 μm grain size and 17.5 g of the fiber was melt-blended with 7.5 g PCL using the Brabender Extruder (Brabender GmbH & Co. KG, Duisburg, Germany) for 15 minutes at 65˚C to prepare the composite of total mass 25 g. By applying a pressure of 110 kg/cm^2, 8.33 g portions of the blended composite were then hot-pressed into 6 cm × 3.6 cm × 0.20 cm flat blocks. The choice of OPEFB fiber to PCL ratio of 7:3 was to ensure that more fiber was used while the ability of the extruder to mix the materials uniformly was not compromised during the melt-blending process.

2.3. Preparation of the Multi-Layered Composites

As shown in **Figure 1**, the multi-layered composites were prepared by inserting each of the 6 cm × 3.6 cm × 0.20 cm recycled α-Fe_2O_3/PCL composites between two layers of the 6 cm × 3.6 cm × 0.20 cm OPEFB fiber/PCL composites before

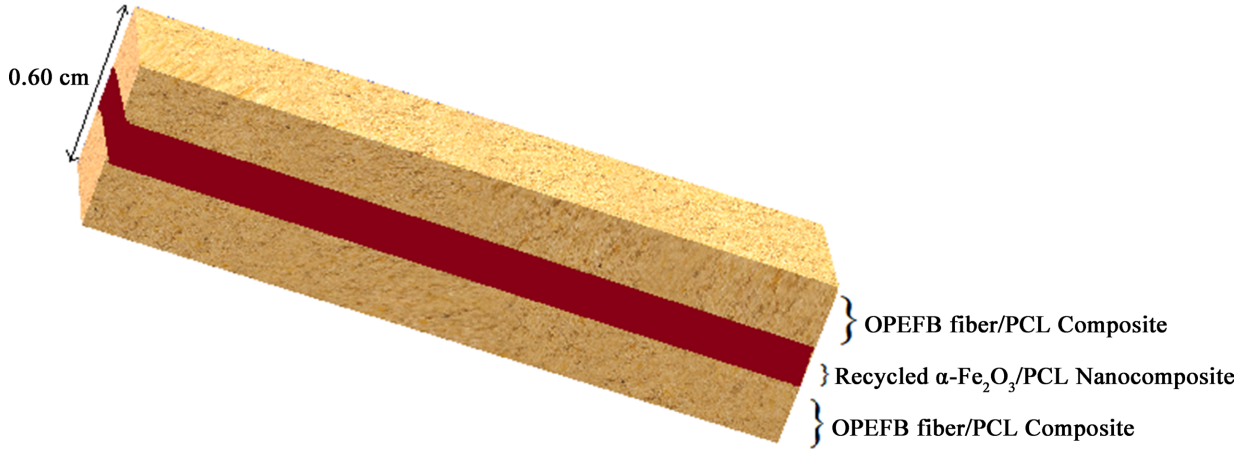

Figure 1. Structure of recycled α-Fe_2O_3/OPEFB fiber/PCL multi-layered composite.

placing in a 6 cm × 3.6 cm × 0.70 cm mold and hot-pressed at a pressure of 110 kg/cm^2 to a final thickness of 0.60 cm and mass 25 g.

3. Characterization

3.1. Morphology

The distribution of the OPEFB fiber and recycled α-Fe_2O_3 nanoparticles within the PCL matrix was examined using the Field Emission Scanning Electron Microscope (JEOL JSM-7600 FESEM, JEOL, Tokyo, Japan).

3.2. Relative Complex Permittivity

The relative complex permittivity values (real, ε'; imaginary, ε'') of all the samples were determined at room temperature by means of the OEC probe connected to a Vector Network Analyzer (Agilent N5230A PNA-L, Agilent Technologies, Santa Clara, USA) and measurements were taken in the microwave frequency range of 1 - 4 GHz. The measurements were obtained by pressing the coaxial probe firmly onto the broader surfaces of the samples while ensuring that there were no air spaces or gaps between the surfaces in contact.

3.3. Microwave Absorption

The reflection coefficient magnitudes ($|S_{11}|$) of the composites were determined theoretically from the Finite Element Method performed on COMSOL Multiphysics software version 3.5 (COMSOL AB, Stockholm, Sweden) based on the microstrip model geometry. The model consisted of a tetrahedral element/mesh of an R/T Duroid 5880 dielectric substrate (length = 6.0 cm, width = 5.0 cm, thickness = 0.15 cm) having a signal line (6.0 cm × 0.15 cm) imprinted along its broader side. The measured ε' and ε'' values of the composites were fed into the software as inputs for the calculation of the $|S_{11}|$ in the 1 - 4 GHz range. To visualize the electric field distribution within the composites, arrow representations of the simulated x-component (V/m) of the field were subsequently obtained after performing parametric analysis at 4 GHz.

4. Results and Discussion

4.1. Morphology

The respective distributions of OPEFB fiber and recycled α-Fe_2O_3 nanoparticles within the PCL matrix was examined from the FESEM micrographs of the surface morphologies of the composites depicted in Figure 2. The micrograph presented in Figure 2(a) for the OPEFB fiber/PCL blend shows no agglomeration, implying that there was an even distribution of the fiber throughout the PCL matrix. The micrographs in Figures 2(b)-(d) represent the surface morphologies of selected recycled α-Fe_2O_3/PCL composites with 5 wt%, 15 wt% and 25 wt% of the recycled α-Fe_2O_3 nanoparticles respectively.

A careful examination of the micrographs shows an even dispersal of bright spots which can be attributed to recycled α-Fe_2O_3 due to its higher atomic number contrast as compared to the PCL matrix. The intensity of the dispersal,

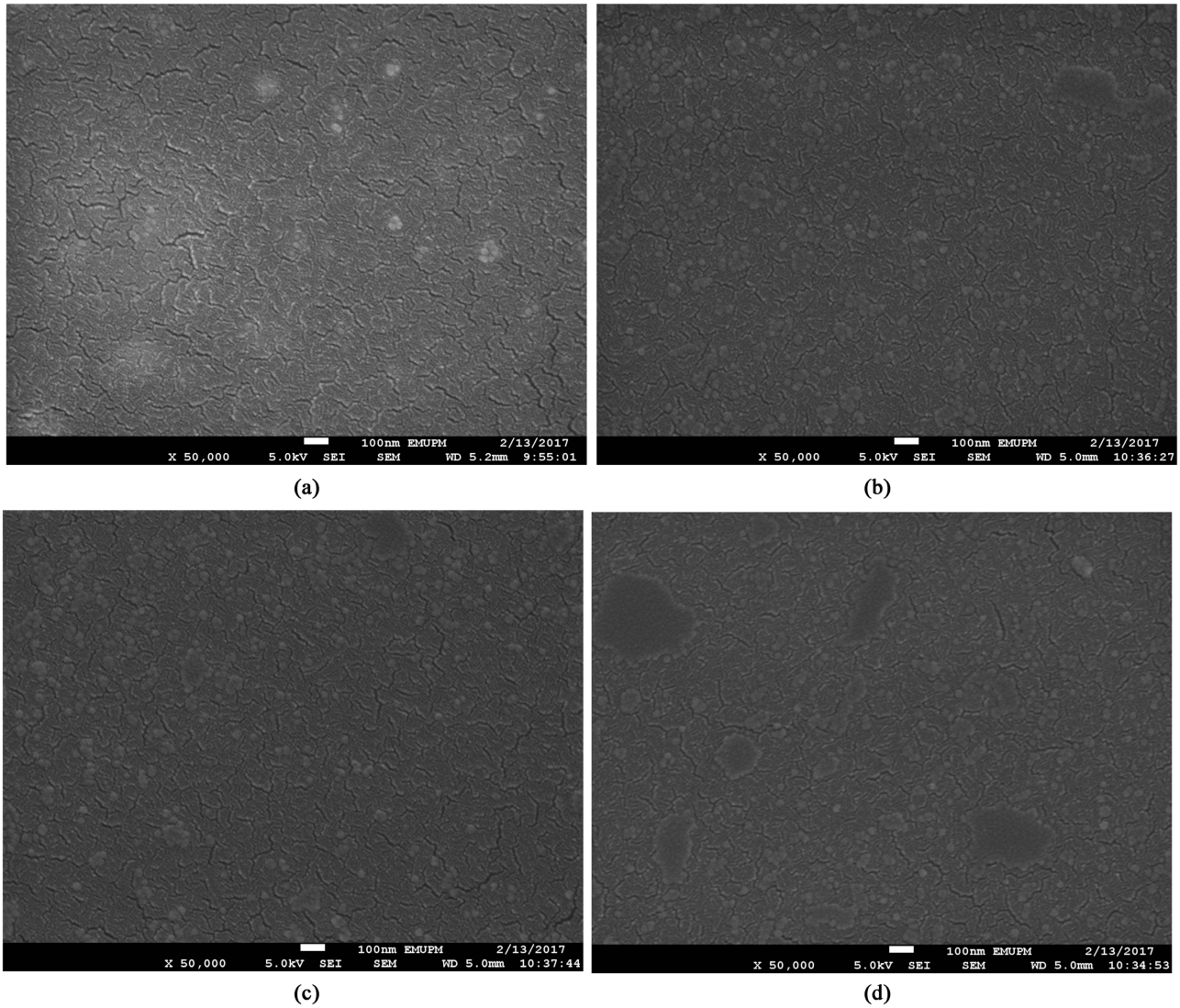

Figure 2. FESEM micrographs of (a) OPEFB fiber/PCL composite; (b) 5 wt% recycled α-Fe_2O_3/PCL composite; (c) 15 wt% recycled α-Fe_2O_3/PCL composite; (d) 25 wt% recycled α-Fe_2O_3/PCL composite.

which increased with the recycled α-Fe_2O_3 nanofiller content, was without agglomeration for all the composites. The homogeneous distribution of the OPEFB fiber and recycled α-Fe_2O_3 nanoparticles in the PCL matrix indicates that they were fully integrated in the composites to provide the interfacial bonding which enhanced the permittivity properties of the composites.

4.2. Relative Complex Permittivity

The relative complex permittivity properties of the composites were determined from the $\varepsilon'$and ε''values using the OEC technique in the frequency range of 1 - 4 GHz. As presented in **Figure 3** and **Figure 4** respectively, the variation in $\varepsilon'$and ε''clearly depict increasing values with recycled α-Fe_2O_3 nanofiller content for all the composites. The ε' values obtained were between 3.0 and 3.9 while the ε'' values ranged between 0.26 and 0.64. For instance, at 2.4 GHz, the ε'values were 3.2, 3.3, 3.4, 3.5 and 3.7 while the ε''values were 0.29, 0.37, 0.40, 0.46 and 0.54 for the 5 wt%, 10 wt%, 15 wt%, 20 wt% and 25 wt% composites respectively.

Since $\varepsilon'$and ε''values largely depend on contributions from orientation, interfacial, electronic and atomic and polarizations [21], the combined utilization of OPEFB fiber and recycled α-Fe_2O_3 nanofiller in the PCL matrix enabled orientation polarization [22] and interfacial polarization [23] respectively to dominate causing the observed increase in the permittivity values. These results therefore suggest that the relative complex permittivity properties of the composites could

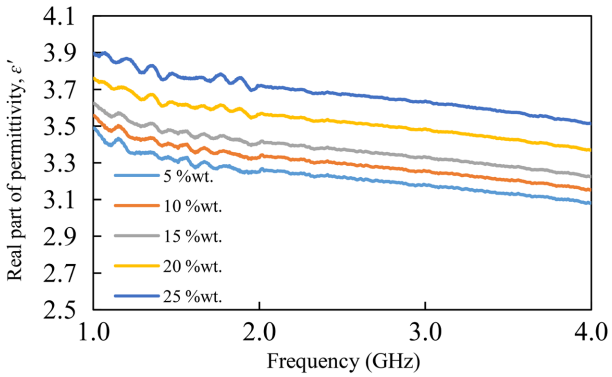

Figure 3. Variation in real part of permittivity with frequency.

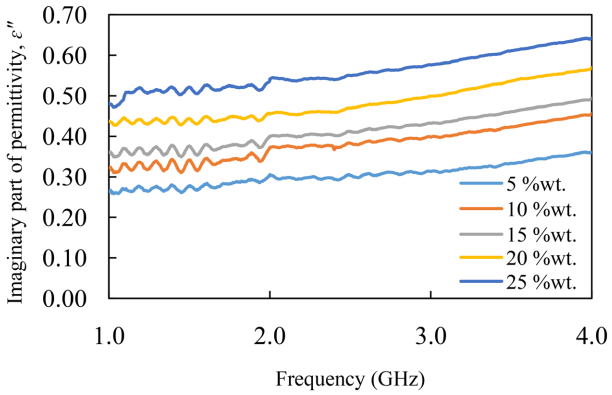

Figure 4. Variation in imaginary part of permittivity with frequency.

be enhanced by increasing the recycled α-Fe_2O_3 nanofiller content, in view of the constant composition of OPEFB fiber. This is consistent with previous studies where the complex permittivity of polymer-based composites increased when fillers having high $\varepsilon'$and ε''values were utilized [1] [10] [24] [25].

A comparison of the measured $\varepsilon'$and ε''values with those of some composites synthesized from ferrites, epoxy and carbon nanotubes is presented in **Table 1**. At the stated frequencies, the ε' of the 25 wt% recycled α-Fe_2O_3/OPEFB fiber/PCL multi-layered composite appears to be comparable to that of 0.01 wt% CNT + epoxy + CoO (3 mm thick) composite but lower than the remaining composites.

However, the ε''values are much higher than the other composites, suggesting that the 25 wt% recycled α-Fe_2O_3/OPEFB fiber/PCL multi-layered composite could serve as an appropriate substitute since materials with high ε''values tend to possess higher absorption properties making them capable of attenuating electromagnetic waves.

Additionally, the effect of the recycled α-Fe_2O_3 nanofiller content on the microwave absorption tendencies of the composites was preliminarily evaluated from the variation of loss tangent (Tan δ) with frequency. As shown in **Figure 5**, the profiles depict a clear linear correlation between absorption properties and increase in recycled α-Fe_2O_3 nanofiller composition for all the composites. For instance, at 2.4 GHz, a strong correlation between loss tangent and fractional composition (x) of the recycled α-Fe_2O_3 nanofiller (**Figure 6**) was observed, indicating that higher absorption could be attained by increasing the nanofiller content beyond 25 wt%.

Table 1. Comparison of $\varepsilon'$and ε''at some specified frequencies.

Material	2 GHz		4 GHz		Reference
	ε'	ε''	ε'	ε''	
0.01 wt% CNT + epoxy + CoO (3.5 mm thick)	3.5	0.30	3.5	0.25	[26]
0.01 wt% CNT + epoxy + CuO (3.5 mm thick)	4.2	0.40	4.1	0.41	[26]
U-type barium hexaferrite-epoxy composite	4.5 - 5.2	<0.30	4.7 - 5.0	<0.30	[4]
α-Fe_2O_3 + OPEFB fiber + PCL multilayered composite (25 wt%, 6 mm thick)	3.7	0.54	3.5	0.64	This study

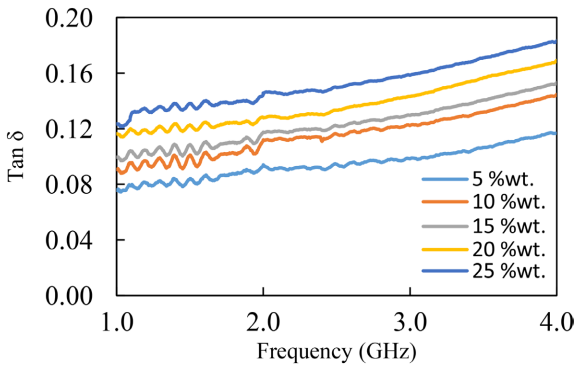

Figure 5. Variation in Tan δ (loss tangent) with frequency.

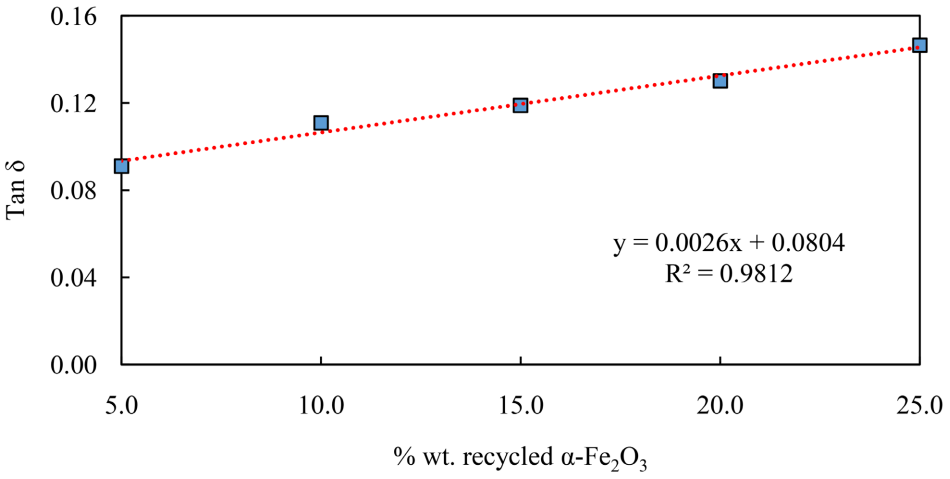

Figure 6. Tan δ (loss tangent) variation with fractional composition (x) of the recycled α-Fe_2O_3 nanofiller at 2.4 GHz.

4.3. Microwave Absorption

The microwave absorbing properties of the composites were examined from the reflection loss (*RL*) values calculated from the expression [27];

$$RL = 20\log|S_{11}|$$

$|S_{11}|$ represents the magnitude of the reflection coefficient of the composites theoretically calculated using the Finite Element Method. **Figure 7** shows a positive correlation between the *RL* (dB) values and increases in recycled α-Fe_2O_3 nanofiller content within the stated frequency range. Generally, the values were all lower than −10 dB, which suggests that all the composites can be predicted to possess 90% microwave absorption capabilities in the 1 - 4 GHz frequency range. The most prominent *RL* (dB) values were located in the 1.38 - 1.46 GHz band with a minimum value of −38 dB attained by the 25 wt% composite. A secondary set of minimum values were also obtained for the 15 wt% - 25 wt% composites in the 2.39 - 3.49 GHz with the lowest of −25 dB at 2.8 GHz.

The predicted high absorption properties of the composites could be attributed to their high ε''values resulting from the enhanced interfacial polarization

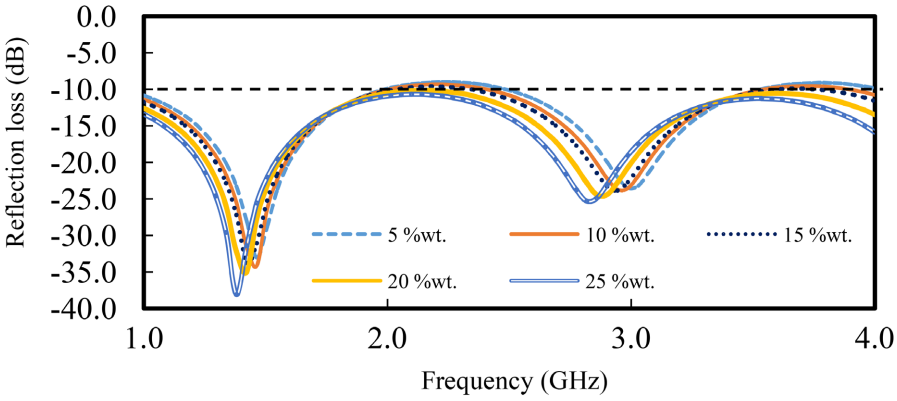

Figure 7. Variation in RL (dB) with frequency.

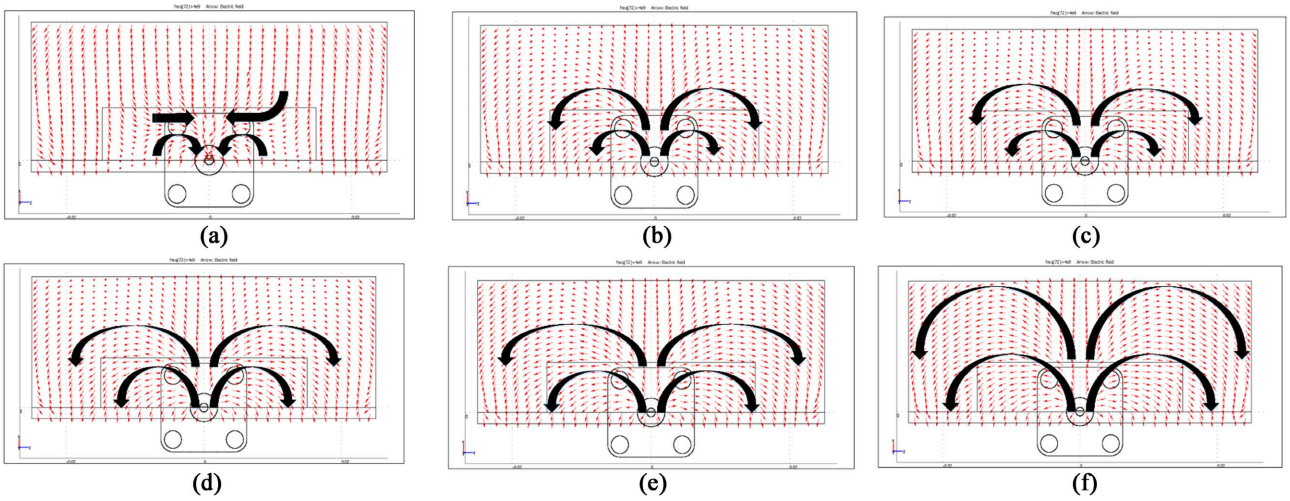

Figure 8. Electric field distribution patterns for: (a) unloaded microstrip; (b) 5 wt%; (c) 10 wt%; (d) 15 wt%; (e) 20 wt%; (f) 25 wt% composites.

due to the combination of the OPEFB fiber and recycled α-Fe_2O_3 nanofiller. These simulated results demonstrate that the recycled α-Fe_2O_3/OPEFB fiber/PCL multi-layered composites can significantly absorb microwaves and would also be environmentally friendly and cheaper alternatives for applications in the 1 - 4 GHz.

In order to visualize the distribution of the electric field within the composites to assess their absorbing properties, the x-component (V/m) of the field was simulated and its direction away from the conducting strip analyzed at 4 GHz using arrows. As depicted in **Figure 8(a)**, the arrows for the unloaded microstrip shows a scattered electric field distribution array particularly in the immediate vicinity of the conducting strip located at the center. However, each of the sample-loaded microstrip shown in **Figures 8(b)-(f)** demonstrates symmetrically and equally dispersed electric field directions alongside the conducting strip line that projects upwards and then back to ground. By increasing the recycled α–Fe_2O_3 nanofiller content, the size of the electric field returning to ground becomes smaller due to absorption. This result is very much consistent with **Figure 4** in the sense that, the higher the ε''values of the composites the fewer the electric field that is distributed to ground as a result of absorption. The simulation of the electric field distribution therefore indicates that the composites are capable of absorbing microwaves in the 1 - 4 GHz region.

5. Conclusion

In this study, 6 mm thick recycled α-Fe_2O_3/OPEFB fiber/PCL multi-layered composites were successfully prepared and investigated for their complex permittivity and microwave absorption properties in 1 - 4 GHz. The results showed that the relative complex permittivity properties of the composites increased linearly with recycled α-Fe_2O_3 nanofiller content and the ε'values obtained varied between 3.0 and 3.9 while the ε''values ranged between 0.26 and 0.64 within 1 - 4

GHz. Additionally, a strong correlation between loss tangent and fractional composition of the recycled α-Fe_2O_3 nanofiller was established at 2.4 GHz which indicated that higher absorption could be attained by increasing the nanofiller content beyond 25 wt% The Reflection loss (dB) of the composites showed the most prominent values within the 1.38 - 1.46 GHz band with a minimum of −38 dB attained by the 25 wt% composite. Another batch of minimum values was also obtained in the 2.39 - 3.49 GHz with the lowest of −25 dB at 2.8 GHz. The recycled α-Fe_2O_3/OPEFB fiber/PCL multi-layered composite are promising materials that can be engineered for solving low frequency (below 4 GHz) noise problems while inherently providing low density, low-cost and environmental benefits.

Acknowledgements

The authors wish to thank the Institute of Advanced Materials (ITMA), UPM for the use of the material synthesis and characterization laboratory and the Department of Physics, UPM for providing access to the RF/microwave laboratory.

Conflicts of Interest

The authors declare no conflicts of interest regarding the publication of this paper.

References

[1] Ahmad, A.F., Abbas, Z., Obaiys, S.J., Ibrahim, N.A., Zainuddin, M.F. and Salem, A. (2016) Permittivity Properties of Nickel Zinc Ferrite-Oil Palm Empty Fruit Bunch-Polycaprolactone Composite. *Procedia Chemistry*, **19**, 603-610. https://doi.org/10.1016/j.proche.2016.03.059

[2] Phor, L. and Kumar, V. (2020) Structural, Thermomagnetic and Dielectric Properties of $Mn_{0.5}Zn_{0.5}Gd_xFe_{2-x}O_4$ (x=0, 0.025, 0.050, 0.075 and 0.1). *Journal of Advanced Ceramics*, **9**, 243-254. https://doi.org/10.1007/s40145-020-0364-y

[3] Rostami, M., Hossein, M. and Ara, M. (2019) The Dielectric, Magnetic and Microwave Absorption Properties of Cu—Substituted Mg-Ni Spinel Ferrite—MWCNT Nanocomposites. *Ceramics International*, **46**, 7606-7613. https://doi.org/10.1016/j.ceramint.2019.01.056

[4] Pratap, V., Soni, A.K., Dayal, S., Abbas, S.M., Siddiqui, A.M. and Prasad, N.E. (2018) Electromagnetic and Absorption Properties of U-Type Barium Hexaferrite-Epoxy Composites. *Journal of Magnetism and Magnetic Materials*, **465**, 540-545. https://doi.org/10.1016/j.jmmm.2018.06.027

[5] Kaur, T., Kumar, S., Hamid, B. and Basharat, B. (2015) Effect on Dielectric, Magnetic, Optical and Structural Properties of Nd-Co Substituted Barium Hexaferrite Nanoparticles. *Applied Physics A*, **119**, 1531-1540. https://doi.org/10.1007/s00339-015-9134-z

[6] Afghahi, S.S.S., Jafarian, M. and Atassi, Y. (2016) A Promising Lightweight Multicomponent Microwave Absorber Based on Doped Barium Hexaferrite/Calcium Titanate/Multiwalled Carbon Nanotubes. *Journal of Nanoparticle Research*, **18**, Article No. 192. https://doi.org/10.1007/s11051-016-3499-6

[7] Shen, P., Luo, J., Zuo, Y., Yan, Z. and Zhang, K. (2017) Effect of La-Ni Substitution

on Structural, Magnetic and Microwave Absorption Properties of Barium Ferrite. *Ceramics International*, **43**, 4846-4851. https://doi.org/10.1016/j.ceramint.2016.12.107

[8] Zhang, K., Gao, X., Zhang, Q., Chen, H. and Chen, X. (2017) Fe_3O_4 Nanoparticles Decorated MWCNTs @ C Ferrite Nanocomposites and Their Enhanced Microwave Absorption Properties. *Journal of Magnetism and Magnetic Materials*, **452**, 55-63. https://doi.org/10.1016/j.jmmm.2017.12.039

[9] Nasser, N., Atassi, Y., Salloum, A., Charba, A. and Malki, A. (2018) Comparative Study of Microwave Absorption Characteristics of Polyaniline/NiZn Ferrite Nanocomposites with Different Ferrite Percentages. *Materials Chemistry and Physics*, **211**, 79-87. https://doi.org/10.1016/j.matchemphys.2018.02.017

[10] Lakin, I.I., Abbas, Z., Azis, R.S. and Alhaji, I.A. (2020) Complex Permittivity and Electromagnetic Interference Shielding Effectiveness of Opefb Fiber-Polylactic Acid Filled with Reduced Graphene Oxide. *Materials*, **13**, Article No. 4602. https://doi.org/10.3390/ma13204602

[11] Abdalhadi, D.M., Abbas, Z., Ahmad, A.F. and Ibrahim, N.A. (2017) Determining the Complex Permittivity of Oil Palm Empty Fruit Bunch Fibre Material by Open-Ended Coaxial Probe Technique for Microwave Applications. *BioResources*, **12**, 3976-3991. https://doi.org/10.15376/biores.12.2.3976-3991

[12] Ahmad, A., Abbas, Z., Obaiys, S. and Abdalhadi, D. (2017) Improvement of Dielectric, Magnetic and Thermal Properties of OPEFB Fibre-Polycaprolactone Composite by Adding Ni-Zn Ferrite. *Polymers*, **9**, Article No. 12. https://doi.org/10.3390/polym9020012

[13] Xie, Y., Kocaefe, D., Chen, C. and Kocaefe, Y. (2016) Review of Research on Template Methods in Preparation of Nanomaterials. *Journal of Nanomaterials*, **2016**, Article ID: 2302595. https://doi.org/10.1155/2016/2302595

[14] Kefeni, K.K., Msagati, T.A.M. and Mamba, B.B. (2017) Ferrite Nanoparticles : Synthesis, Characterisation and Applications in Electronic Device. *Materials Science & Engineering*: *B*, **215**, 37-55. https://doi.org/10.1016/j.mseb.2016.11.002

[15] Azis, R.S., Hashim, M., Saiden, N.M., Daud, N. and Shahrani, N.M.M. (2016) Study the Iron Environments of the Steel Waste Product and Its Possible Potential Applications in Ferrites. *Advanced Materials Research*, **1109**, 295-299. https://doi.org/10.4028/www.scientific.net/AMR.1109.295

[16] Shahrani, N.M.M., Azis, R.S., Hashim, M., Hassan, J., Zakaria, A. and Daud, N. (2016) Effect of Variation Sintering Temperature on Magnetic Permeability and Grain Sizes of $Y_3Fe_5O_{12}$ Via Mechanical Alloying Technique. *Materials Science Forum*, **846**, 395-402. https://doi.org/10.4028/www.scientific.net/MSF.846.395

[17] Mensah, E.E., Abbas, Z., Azis, R.S. and Khamis, A.M. (2019) Enhancement of Complex Permittivity and Attenuation Properties of Recycled Hematite (α-Fe_2O_3) Using Nanoparticles Prepared Via Ball Milling Technique. *Materials*, **12**, Article No. 1696. https://doi.org/10.3390/ma12101696

[18] Du, M., Yao, Z., Zhou, J., Liu, P., Yao, T. and Yao, R. (2017) Design of Efficient Microwave Absorbers Based on Multi-Layered Polyaniline Nanofibers and Polyaniline Nanofibers/$Li_{0.35}Zn_{0.3}Fe_{2.35}O_4$. *Synthetic Metals*, **223**, 49-57. https://doi.org/10.1016/j.synthmet.2016.11.039

[19] Jafarian, M., Afghani, S.S.S., Atassi, Y. and Salehi, M. (2019) Insights on the Design of a Novel Multicomponent Microwave Absorber Based on $SrFe_{10}Al_2O_{19}$ and $Ni_{0.5}Zn_{0.5}Fe_2O_4$/MWCNTs/Polypyrrole. *Journal of Magnetism and Magnetic Materials*, **471**, 30-38. https://doi.org/10.1016/j.jmmm.2018.09.047

[20] Liu, P., Ng, V.M.H., Yao, Z., Zhou, J., Lei, Y., Yang, Z. and Kong, L.B. (2017) Microwave Absorption Properties of Double-Layer Absorbers Based on $Co_{0.2}Ni_{0.4}Zn_{0.4}Fe_2O_4$ Ferrite and Reduced Graphene Oxide Composites. *Journal of Alloys and Compunds*, **701**, 841-849. https://doi.org/10.1016/j.jallcom.2017.01.202

[21] Sreekumar, P., Saiter, J.M., Joseph, K., Unnikrishnan, G. and Thomas, S. (2012). Electrical Properties of Short Sisal Fiber Reinforced Polyester Composites Fabricated by Resin Transfer Molding. *Composites Part A*: *Applied Science and Manufacturing*, **43**, 507-511. https://doi.org/10.1016/j.compositesa.2011.11.018

[22] Pickering, K.L., Efendy, M.G.A. and Le, T.M. (2016) A Review of Recent Developments in Natural Fibre Composites and Their Mechanical Performance. *Composites Part A*: *Applied Science and Manufacturing*, **83**, 98-112. https://doi.org/10.1016/j.compositesa.2015.08.038

[23] Mandal, S.K., Singh, S., Dey, P., Roy, J.N., Mandal, P.R. and Nath, T.K. (2016) Frequency and Temperature Dependence of Dielectric and Electrical Properties of TFe_2O_4 (T=Ni, Zn, $Zn_{0.5}Ni_{0.5}$) Ferrite Nanocrystals. *Journal of Alloys and Compounds*, **656**, 887-896. https://doi.org/10.1016/j.jallcom.2015.10.045

[24] Moučka, R., Lopatin, A.V., Kazantseva, N.E., Vilčáková, J. and Sáha, P. (2007) Enhancement of Magnetic Losses in Hybrid Polymer Composites with MnZn-Ferrite and Conductive Fillers. *Journal of Materials Science*, **42**, 9480-9490. https://doi.org/10.1007/s10853-007-2081-0

[25] Chen, D., Quan, H., Huang, Z., Luo, S., Luo, X., Deng, F., Jian, H. and Zeng, G. (2014) Electromagnetic and Microwave Absorbing Properties of RGO@hematite Core-Shell Nanostructure/PVDF Composites, *Composite Science and Technology*, **102**, 126-131. https://doi.org/10.1016/j.compscitech.2014.06.018

[26] Micheli, D., Pastore, R., Del, A., Giusti, A., Vricella, A., Santoni, F., Marchetti, M., Tolochko, O. and Vasilyeva, E. (2017) Electromagnetic Characterization of Advanced Nanostructured Materials and Multilayer Design Optimization for Metrological and Low Radar Observability Applications. *Acta Astronautica*, **134**, 33-40. https://doi.org/10.1016/j.actaastro.2017.01.044

[27] Widanarto, W., Ardenti, E., Ghoshal, S.K., Kurniawan, C., Effendi, M. and Cahyanto, W.T. (2018) Significant Reduction of Saturation Magnetization and Microwave-Reflection Loss in Barium-Natural Ferrite via Nd^{3+} Substitution. *Journal of Magnetism and Magnetic Materials*, **456**, 288-229. https://doi.org/10.1016/j.jmmm.2018.02.050